Local Field Effects in the Electron Energy Loss Spectra of Rutile TiO_2

Nathalie Vast,[1] Lucia Reining,[1] Valerio Olevano,[1] Peter Schattschneider,[2] and Bernard Jouffrey[3]
[1]*Laboratoire des Solides Irradiés, CNRS-CEA, École Polytechnique, F-91128 Palaiseau, France*
[2]*Institut für Angewandte und Technische Physik, University of Technology Vienna, A-1040 Vienna, Austria*
[3]*LMSS-MAT, CNRS-UMR 8579, École Centrale Paris, F-92295 Châtenay-Malabry, France*

(Received 30 May 2001; published 3 January 2002)

We present an *ab initio* calculation of the electron energy loss spectrum of rutile TiO_2 in the energy range of 0 to 60 eV, focusing our interest on the excitation from the titanium $3p$ semicore levels. The results are compared to our measurements. Local field effects turn out to be crucial at those energies, and their inclusion in the calculation yields excellent agreement between theory and experiment. We show how in rutile these effects induce an anisotropy in the otherwise isotropic transitions from quasispherical $3p$ semicore states to $3d$ states of almost cubic symmetry.

DOI: 10.1103/PhysRevLett.88.037601 PACS numbers: 79.20.Uv, 71.15.Mb, 77.22.–d, 77.84.Bw

Electron energy loss spectroscopy (EELS) is increasingly used for the investigation of materials. Spectra can be obtained at variable momentum transfer and complex problems like bonding in metals and alloys [1] or local environments at interfaces [2] can be investigated.

Excitations from core levels are generally compared either to the results of atomistic scattering approaches based on the evaluation of the scattering probabilities and phase shifts of the incident electron in the potential of the target [3], or to the density of unoccupied states obtained in an *ab initio* supercell calculation, simulating the core hole as a positive charge—the $Z + 1$ approximation [4]—or treating it self-consistently [5].

In the energy range of valence transitions, the dispersion of the initial states cannot be neglected, and transition matrix elements must be explicitly calculated. To this end, one usually uses the random phase approximation (RPA), where the microscopic dielectric function ε is constructed from the band structure according to

$$\varepsilon_{\mathbf{G},\mathbf{G}'}(\mathbf{q},\omega) = \delta_{\mathbf{G},\mathbf{G}'} - v(\mathbf{q}+\mathbf{G})\chi^0_{\mathbf{G},\mathbf{G}'}(\mathbf{q},\omega). \tag{1}$$

$\mathbf{G}$ is a reciprocal lattice vector, $\mathbf{q}$ is a vector in the first Brillouin zone, v is the bare Coulomb interaction, and the independent-particle response function χ^0 is a sum over transitions between occupied and empty states [6]. The transition energies and matrix elements are often obtained from the eigenvalues and eigenfunctions of the Kohn-Sham equation of density functional theory (DFT) [7]. Then, one constructs the energy loss function $-\mathrm{Im}[\varepsilon^{-1}_{\mathbf{G},\mathbf{G}'}(\mathbf{q},\omega)]_{\mathbf{G}=\mathbf{G}'=0}$. Since the crystal is inhomogeneous, it is important to consider the so-called crystal local-field effects (LFE). One possible way is to take into account the off-diagonal elements of the dielectric matrix $\varepsilon_{\mathbf{G},\mathbf{G}'}(\mathbf{q},\omega)$ in the matrix inversion. These effects have a strong influence on the valence plasmon position and line shape [8], and they are even more important at higher energies, where more localized states are contributing. For instance, LFE have been shown to be large for the deep-level x-ray absorption spectra of transition metals [9]. So far, we are not aware of studies concentrating on the intermediate energy range of semicore levels.

Those energies are, however, interesting, e.g., in various compounds of $3d$ transition metals, where the $3p$ states are almost atomiclike, but still feel the interaction with neighboring atoms and do in general slightly hybridize. A good case to study is TiO_2, a relatively simple transition metal oxide with titanium $3p$ semicore levels at intermediate energy, about 33 eV below the upper valence band. It also meets a broad technological interest, due to its application in photocatalysis [10] and in paint.

The aim of this work is to study LFE in the EELS spectra of rutile TiO_2, in an energy range of up to 60 eV, which covers the transitions from valence and semicore states. We show that this can be done by performing *ab initio* plane wave calculations, using the fact that charge fluctuations of high spatial frequency can be neglected. LFE in the semicore region are found to be strong. It is particularly interesting to see how the anisotropy of the rutile crystal shows up even in transitions from the almost spherical semicore levels: in fact, LFE introduce the "surroundings" in an otherwise local measurement. We confirm our calculations by performing EELS measurements on a rutile single crystal, and obtain excellent agreement when LFE and the geometry of the experiment are included in the comparison.

Our calculations start with a DFT ground state calculation within the local density approximation (LDA). We use norm-conserving pseudopotentials [11], a plane wave basis and, due to the inclusion of the $3s$ and $3p$ semicore states, an energy cutoff of 140 Ry. We determine the equilibrium lattice parameters for the rutile crystal to be $a = 4.52$ and $c = 2.91$ Å, in excellent agreement with the experimental results $a_{\mathrm{exp}} = 4.59$ and $c_{\mathrm{exp}} = 2.96$ Å [12]. Next, we construct χ^0 and ε [Eq. (1)]. To compute the EELS spectrum without LFE, we need one sole diagonal element, $\varepsilon_{\bar{\mathbf{G}},\bar{\mathbf{G}}}(\mathbf{q},\omega)$, if we are interested in a momentum transfer $\mathbf{q} + \bar{\mathbf{G}}$. Here $\bar{\mathbf{G}} = \mathbf{0}$.

The bottom panel of Fig. 1 shows our calculated loss function for vanishing $\mathbf{q}$ neglecting LFE. For the

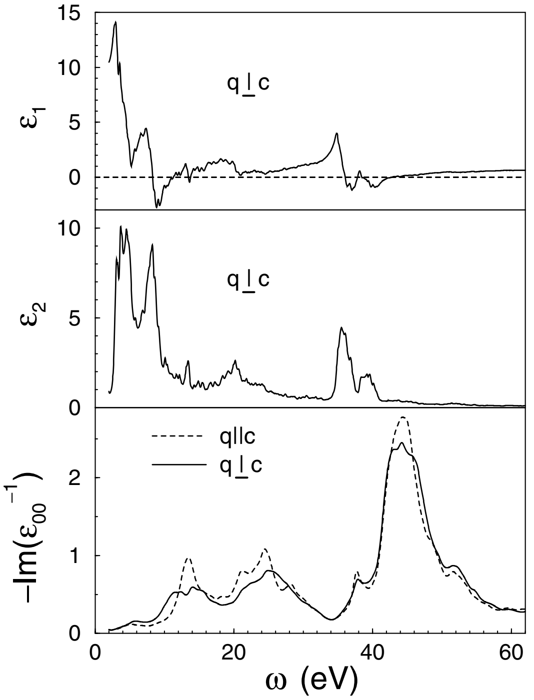

FIG. 1. Theoretical spectra without LFE at $\mathbf{q} = \mathbf{0}$. Upper (central) panel: real (imaginary) part of the dielectric function, with a Lorentzian broadening (LB) of 0.1 eV. Lower panel: corresponding loss function, with a LB of 0.6 eV.

continuous (dashed) line, $\mathbf{q}$ has been taken perpendicular (parallel) to the c axis, yielding a dielectric function called $\varepsilon_\perp(\varepsilon_\|)$ below. The upper panel of Fig. 1 shows the real part of $\varepsilon_\perp$, ε_1, and the central panel its imaginary part, ε_2. We identify three principal structures in the loss function, $\varepsilon_2/(\varepsilon_1^2 + \varepsilon_2^2)$: first, a structured plasmon peak at about 13 eV, caused by the double zero of ε_1; second, a broad collective excitation at about 25 eV stemming from a small linearly increasing real part and a linearly decreasing imaginary part. This low energy part is in qualitative agreement with the calculations of Ref. [13]. Third, transitions from the Ti $3p$ levels to the lowest conduction bands—coming from $3d$ atomic states—form two peaks at 35 and 39 eV in ε_2 [14]. These empty states have quasicubic t_{2g} and e_g character, indicating the smallness of the tetragonal perturbation induced by the D_{4h} crystal field. They cause the double zero in ε_1, hence the double peak at about 37.7 and 44.4 eV in the loss function. The double peak shows substructures in both polarizations, which is characteristic of $3p$ to $3d$ transitions and has been observed and explained by multiplets approaches, e.g., in the EELS of TiN, or in the $M_{2,3}$ absorption spectra of TiF_3 [15]. Although the present calculation reveals a dispersion of 0.7 eV for the Ti $3p$ bands, this energy level is in a certain sense atomiclike: whereas the height of the valence plasmon peak increases by almost 50% when going from $\mathbf{q}\perp c$ to $\mathbf{q}\| c$, together with a change in line shape, the height of the semicore peaks at 37.7 and 44.4 eV increases by only 12%, and little change in line shape is found. This is a consequence of the almost spherical symmetry of the quasidegenerate p levels and of the quasicubic symmetry of the narrow final states.

In order to include LFE, one possibility is to calculate the *whole* dielectric matrix, and invert it for every frequency ω which, in view of the many plane waves (PW's) in the basis, would be in principle an impossible task. However, it turns out that the size of the matrix to be inverted can be chosen much smaller than the number of PW's for the wave functions. Figure 2 shows the same quantities as Fig. 1, but including LFE. The continuous and dashed curves have been obtained at full convergence, using only 327 PW's in the matrix inversion—compared to the 2000 PW's which are needed for the calculation of the matrix elements. Moreover, the dot-dashed curve in the inset also shows the result for a calculation using only 137 PW's, i.e., with $|G| < 5$ Å^{-1}. It can be seen (i) that LFE, as we expected, drastically reduce the peak heights, changing both positions and line shapes, and *cannot* be neglected but (ii) that the main part of the effect can be recovered using very small matrices, which suggests that one should always include these effects. Now let us look again at the asymmetry of the results. Including LFE, the difference between $\varepsilon_\|$ and $\varepsilon_\perp$ is enhanced, and this is particularly evident on the formerly almost isotropic semicore peak. In fact, the previously independent transitions mix, and hence transitions to more anisotropic states contribute to the semicore peak. This mixing could equivalently be described by the concept of an electron-hole exchange interaction [9,16], or when an atomic picture is adequate, by the mixing of multiplets.

From our theoretical results, it is hence clear that LFE play a key role for the quantitative determination of the EELS spectra in the semicore region. In order to show

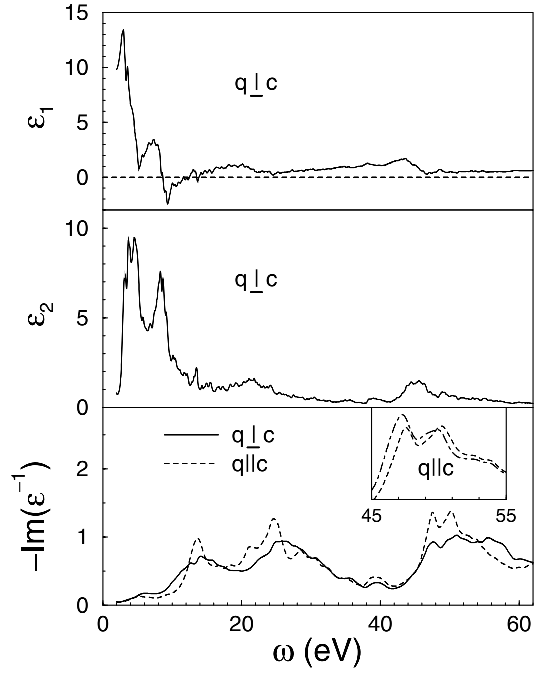

FIG. 2. Same caption as Fig. 1, with LFE. Inset: results with 327 (dashed line) and 127 (dot-dashed line) $\mathbf{G}$ vectors.

that they are actually sufficient, and that we can neglect more complicated many-body effects such as self-energy corrections and the electron-hole attraction [17,18], we have performed experiments with a transmission electron microscope (TEM). The scattering geometry in the TEM allows the detection of the signal in the diffraction plane, i.e., selecting a scattering vector in the reciprocal lattice of the specimen: both a vanishing $\mathbf{q}$ and a $q \approx 0.4$ Å^{-1} in the [110] direction were chosen.

The specimen was prepared by cutting a slab from a single crystal, mechanical thinning and ion milling. It was approximately 100 nm thick. The incident electron beam was oriented parallel to the (001) axis of the rutile crystal. In the first experiment, the scattering angle θ was set to zero, corresponding to $q \approx 0$. In the second experiment we set the spectrometer aperture at (0.5, 0.5, 0) in the diffraction plane, corresponding to a Bragg angle of $\theta = 1.73$ mrad, and to $q_\perp \approx 0.4$ Å^{-1}. Since $q_{\|}$ is small, the scattering vector points almost in the (110) direction.

Experiments were performed at 160 kV acceleration voltage in a Philips CM20 TEM equipped with a LaB$_6$ filament. Spectra were recorded in diffraction mode (image coupling) with a GATAN 666 spectrometer in typically 1 sec for zero scattering angle and 10 sec for $\theta = 1.73$ mrad. The full width at half maximum of the zero-loss peak, giving the energy resolution, was 1.2 eV. After automatic dark count and gain correction, the tail of the zero-loss peak was removed with the standard EL/P routine [19]. The beam was strongly overfocused in order to achieve a sufficiently parallel bundle. The half-angle subtended by the illumination cone was estimated to 0.17 mrad for $q \approx 0$, and 0.78 mrad for $q \approx 0.4$ Å^{-1}. The collection angle subtended at the spectrometer aperture was estimated to be 0.09 mrad for $q \approx 0$, and 0.32 mrad for $q \approx 0.4$ Å^{-1}.

The loss function relates to the double differential inelastic scattering probability for fast electrons as

$$\frac{\partial^2 p}{\partial\Omega\,\partial E} = D\,\frac{4\pi\varepsilon_0}{(e\pi a_0)^2}\,\mathrm{Im}\left(\frac{-1}{\mathbf{q}\bar{\varepsilon}\mathbf{q}}\right), \tag{2}$$

where D is the sample thickness, a_0 is the Bohr radius, $\bar{\varepsilon}$ is the macroscopic dielectric tensor, $\mathbf{q}$ is the scattering vector decomposed into a perpendicular component $q_\perp = k_0 \tan\theta$, and a parallel one $q_{\|} = k_0\theta_E$. k_0 is the incident electron's wave vector, θ is the scattering angle, and $\theta_E = E_{\mathrm{loss}} m/\hbar^2 k_0^2$ is the characteristic angle depending on the energy loss E_{loss} and on the relativistic mass m of the beam electron. When comparing the data obtained at vanishing q, Eq. (2) must be integrated over an experimentally determined angular range β taking into account both the finite aperture of the illuminating system and of the spectrometer. Assuming a Lorentzian angular distribution of the loss function, one obtains [20]

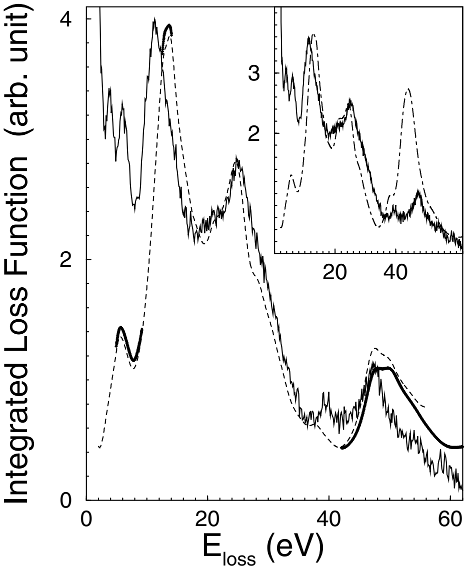

FIG. 3. Integrated loss function at $\mathbf{q} \approx \mathbf{0}$ for $\beta = 0.12$ mrad. Solid line: experiment. Dashed line: TDLDA. Thick line: RPA. For clarity, RPA has been omitted when indistinguishable from TDLDA. Inset: RPA without LFE.

$$I(E) \propto -\mathrm{Im}\left[\frac{\pi}{\varepsilon_\perp(0)}\ln\left(1 + \frac{\beta^2\varepsilon_\perp(0)}{\theta_E^2\varepsilon_{\|}(0)}\right)\right]. \tag{3}$$

Equation (3) was fitted to the experiment, and the best result obtained for $\beta = 0.12$ mrad, within the range of experimental uncertainty of 0.1–0.2 mrad. In Fig. 3, the logarithmic factor suppresses intensity at high energy compared to the loss function of Fig. 2. When LFE are included, the agreement between theory and experiment is excellent, as compared to neglect of LFE (Fig. 3, inset).

In order to study the role of the exchange-correlation contributions, we also report in a dashed line the results obtained within time-dependent DFT in the adiabatic local density approximation (TDLDA [21]). We recall that in this framework, $\varepsilon^{-1} = 1 + v\chi^0[1 - (v + f_{xc})\chi^0]^{-1}$, where the exchange-correlation kernel f_{xc} is the functional derivative of the Kohn-Sham exchange-correlation potential with respect to the density. As found in other systems, the effect is visible only for those structures where strong LFE occur [22]. The plasmon peak and the collective excitation at 25 eV are weakly affected by the inclusion of the exchange-correlation kernel, whereas the semicore peak exhibits a small shift towards lower frequencies and a slight increase of the intensity.

It is expected that LFE increase for increasing $\mathbf{q}$. We have therefore calculated $\varepsilon_\perp(q)$ for q ≈ 0.4 Å^{-1} in the [110] direction. The spectrum without LFE—not shown—yields results which are very similar up to 25 eV to those reported in Fig. 1, apart from a shift of the plasmon peak of 1 eV towards lower frequency. The broad collective excitation at 25 eV hardly changes. To compare to the experiment, the intensity is now obtained from [20]

$$I(E) \propto -\mathrm{Im}\left[\int_0^{2\pi}\int_0^{\beta}\frac{d\phi\,\gamma\,d\gamma}{\theta_E^2\varepsilon_{\|}(0) + (\theta^2 + \gamma^2 + 2\theta\gamma\cos\phi)\varepsilon_\perp(q)}\right], \tag{4}$$

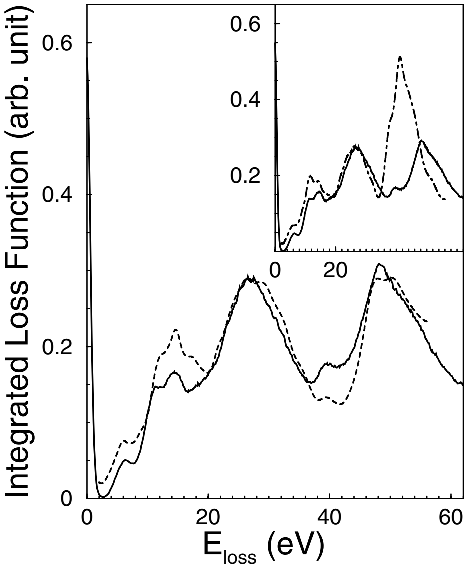

FIG. 4. Integrated loss function at $\mathbf{q} \approx 0.4$ Å^{-1} for $\beta = 1$ mrad. Solid line: Experiment. Dashed line: RPA results. The inset shows the theoretical results without LFE.

where β is 1 mrad. At low energy, the differences seen between the theoretical spectra without LF in the insets of Figs. 3 and 4 thus come from the different experimental geometries expressed in Eqs. (3) and (4). At higher energy the theoretical joint density of states sharply decreases and the main semicore peak drastically changes both in position, now at 41.2 eV, and intensity. LFE reduce even more the intensity and the position of the peak is shifted by more than 6 eV: at 47.3 eV, it is in very good agreement with experiment.

In conclusion, we have calculated and measured the EELS of rutile in the range of 0–60 eV. We find that the inclusion of LFE is particularly important at high energy where transitions from the localized semicore states are involved. TDLDA has only minor consequences on the spectrum, and in view of the very good results, it seems justified to neglect further exchange-correlation effects in that energy range, which means that self-energy and direct electron-hole interaction effects essentially cancel each other. Moreover, we have shown how the anisotropy of the surroundings of an otherwise isotropic localized level influences the resulting spectra when LFE are included. Since it turns out that relatively few spatial frequencies are sufficient to reasonably describe these effects, the calculation of reference spectra for the interpretation of experiments is feasible in a plane wave basis even in the energy range of the semicore levels. Useful information about the structural and chemical environment of the corresponding atoms may therefore be obtained by combining EELS measurements and calculations.

We are grateful to Gilles Hug and Angel Rubio for useful discussions and comments. This work has been supported in part by the European Community Contract No. HPRN-CT-2000-00167 and by the Austrian Science Fund under Project No. P14038-PHY. Travel support by the Austrian ÖAD (Amadée III.5) and the French CNRS (PICS No. 913) is gratefully acknowledged. Computer time has been granted by IDRIS on the NEC SX5.

[1] D. A. Müller, D. J. Singh, and J. Silcox, Phys. Rev. B **57**, 8181 (1998).

[2] S. Nufer, A. G. Marinopoulos, T. Gemming, C. Elsässer, W. Kurtz, S. Köstlmeier, and M. Rühle, Phys. Rev. Lett. **86**, 5066 (2001); D. A. Pankhurst, G. A. Botton, and C. J. Humphreys, Phys. Rev. B **63**, 205117 (2001).

[3] See, e.g., A. J. Scott, R. Brydson, M. MacKenzie, and A. J. Craven, Phys. Rev. B **63**, 245105 (2001); H. R. Moser and G. Wendin, Phys. Rev. B **44**, 6044 (1991).

[4] See, e.g., C. Elsässer and S. Köstlmeier, Ultramicroscopy **86**, 325 (2001).

[5] R. Buczko, G. Duscher, S. J. Pennycook, and S. T. Pantelides, Phys. Rev. Lett. **85**, 2168 (2000).

[6] H. Ehrenreich and M. H. Cohen, Phys. Rev. **155**, 786 (1959).

[7] P. Hohenberg and W. Kohn, Phys. Rev. **136**, B864 (1964); W. Kohn and L. J. Sham, Phys. Rev. **140**, A1133 (1965).

[8] S. G. Louie, J. Chelikowsky, and M. L. Cohen, Phys. Rev. Lett. **34**, 155 (1975); R. Daling, W. van Haeringen, and B. Farid, Phys. Rev. B **45**, 8970 (1992); K. Sturm, Phys. Rev. Lett. **40**, 1599 (1978); Adv. Phys. **31**, 1–64 (1982).

[9] J. Schwitalla and H. Ebert, Phys. Rev. Lett. **80**, 4586 (1998).

[10] R. I. Bickley, Catalysis **5**, 308 (1982); R. Asahi, T. Morikawa, T. Ohwaki, K. Aoki, and Y. Taga, Science **293**, 269 (2001).

[11] M. Fuchs and M. Scheffler, Comput. Phys. Commun. **119**, 67 (1999); D. R. Hamann, Phys. Rev. B **40**, 2980 (1989).

[12] D. T. Cromer and K. Herrington, J. Am. Chem. Soc. **77**, 4708 (1955).

[13] S. D. Mo and W. Y. Ching, Phys. Rev. B **51**, 13 023 (1995).

[14] K. M. Glassford and J. R. Chelikowsky, Phys. Rev. B **46**, 1284 (1992).

[15] G. G. Fuentes *et al.,* Phys. Rev. B **63**, 075403 (2001); T. Yamaguchi, S. Shibuya, S. Suga, and S. Shin, J. Phys. Solid State Phys. **15**, 2641 (1982).

[16] C. Colliex and P. Trebbia, Physica Fennica **9**, S1, 80 (1974).

[17] W. A. Caliebe, J. A. Soininen, E. L. Shirley, C.-C. Kao, and K. Hämäläinen, Phys. Rev. Lett. **84**, 3907 (2000).

[18] V. Olevano and L. Reining, Phys. Rev. Lett. **86**, 5962 (2001).

[19] EL/P 3.0 User's Guide, Gatan, Inc., 1988–1995.

[20] The theoretical intensities reported in Fig. 3 (Fig. 4) are dimensionless. They are the right members of Eq. (3) [Eq. (4)] convoluted with a Lorentzian (0.7 eV + $0.01E_{\mathrm{loss}}$) and a Gaussian ($0.01E_{\mathrm{loss}}$) broadening function.

[21] E. Runge and E. K. U. Gross, Phys. Rev. Lett. **52**, 997 (1984); E. K. U. Gross and W. Kohn, Phys. Rev. Lett. **55**, 2850 (1985).

[22] See, e.g., S. Waidmann, M. Knupfer, B. Arnold, J. Fink, A. Fleszar, and W. Hanke, Phys. Rev. B **61**, 10 149 (2000).